

# Journal of Materials Chemistry B

Accepted Manuscript



This article can be cited before page numbers have been issued, to do this please use: R. Guo, J. Yin, Y. Ma, Q. A. Wang and W. Lin, *J. Mater. Chem. B*, 2018, DOI: 10.1039/C8TB00298C.



This is an Accepted Manuscript, which has been through the Royal Society of Chemistry peer review process and has been accepted for publication.

Accepted Manuscripts are published online shortly after acceptance, before technical editing, formatting and proof reading. Using this free service, authors can make their results available to the community, in citable form, before we publish the edited article. We will replace this Accepted Manuscript with the edited and formatted Advance Article as soon as it is available.

You can find more information about Accepted Manuscripts in the [author guidelines](#).

Please note that technical editing may introduce minor changes to the text and/or graphics, which may alter content. The journal's standard [Terms & Conditions](#) and the ethical guidelines, outlined in our [author and reviewer resource centre](#), still apply. In no event shall the Royal Society of Chemistry be held responsible for any errors or omissions in this Accepted Manuscript or any consequences arising from the use of any information it contains.

## A novel mitochondria-targeted rhodamine analogue for detection of viscosity changes in living cells, zebra fishes and living mice†

Rui Guo,<sup>a</sup> Junling Yin,<sup>b</sup> Yanyan Ma,<sup>b</sup> Qian Wang<sup>a,\*</sup>, and Weiyang Lin<sup>a,b,\*</sup>

Received 00th January 20xx,  
Accepted 00th January 20xx

DOI: 10.1039/x0xx00000x

www.rsc.org/

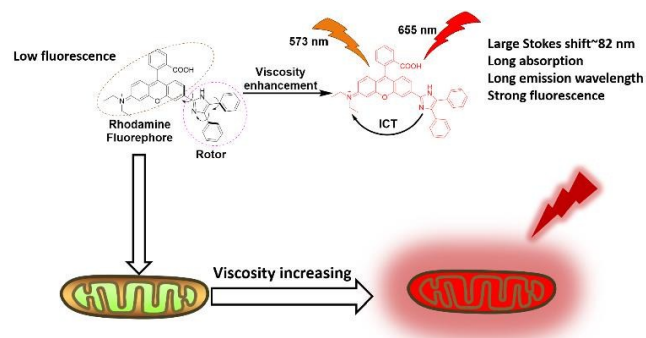
Monitoring the intracellular viscosity changes is crucial to better understand the diffusion-controlled cellular processes. Herein, we synthesized a novel phenyl-substituted imidazole fused rhodamine analogue **RV-1** with long absorption at 573 nm and a large Stokes shift about 82 nm for monitoring the change of cellular viscosity. The new probe **RV-1** showed very strong fluorescence emission at around 655 nm, with a 48.5-fold enhancement of fluorescence intensity from methanol to 99% glycerol. Significantly, the innovative probe **RV-1** was successfully applied for detection of the viscosity change not only in living cells, but also in zebra fishes and living mice.

### Introduction

The cytoplasm of virtually all living cells is highly crowded with intracellular organelles and macromolecules such as proteins, lipids, nucleic acids, and sugars.<sup>1, 2</sup> The consequences of this crowding in cells may hinder the solute diffusion to influence the key cellular functions, including protein folding, enzyme catalysis, intracellular signalling, intracellular transport, and localization of molecules and organelles.<sup>3</sup> One of the primary factors which determine the solute diffusion is viscosity,<sup>4</sup> and therefore, it is crucial to monitor the viscosity changes in various cellular processes. Moreover, Mitochondria, which play critical roles in a number of vital cellular processes, such as ATP production, central metabolism, and apoptosis.<sup>5</sup> Viscosity changes in mitochondria may lead to the dysfunction of the mitochondria. However, measuring the viscosity on the microscopic scale such as in tiny living cells still difficult.<sup>6</sup> The local micro-viscosity in the cells changes widely from one region to another, which is very different to the viscosity observed on a macroscopic scale.<sup>3</sup> Therefore, the methods for detection of the viscosity changes in cells or on subcellular level are still in high demand.

The fluorescence technology becomes a powerful tool

applied in biological field due to its simple operation and high sensitivity as well as the excellent spatial and temporal resolution. A class of fluorescent probes termed fluorescent molecular rotors were developed for detection of the cellular viscosity variations. The molecular rotors are fluorescent molecules with an intramolecular charge transfer (ICT) mechanism undergoing the twisting motion in the excited state.<sup>7</sup> When the molecule absorbs a photon, it first gives a planar excited state with charge transfer, then forms a twisted excited state by intramolecular rotation.<sup>8</sup> The rotation typically leads to a dark non emissive excited state.<sup>9</sup> In low viscous solutions, the fluorescent molecular rotor exhibits very weak fluorescence due to their freely rotation. Whereas, in the high viscous solutions, the rotation of the fluorescent molecular rotor is hindered to emit strong fluorescence emission. There have been numerous fluorescent molecular rotors reported,<sup>10-13</sup> but most of them have short absorption/excitation wavelength in the range of 300-500 nm, which may lead to damage to living biological systems. Therefore, it remains highly desirable for construction of the fluorescent molecular rotors with longer absorption/excitation wavelengths for detection of viscosity in living cells.



Scheme 1 The structure and proposed mechanism of **RV-1** for response to viscosity.

<sup>a</sup>State Key Laboratory of Chemo/Biosensing and Chemometrics, College of Chemistry and Chemical Engineering, Hunan University, Changsha, Hunan 410082, P. R. China

<sup>b</sup>Institute of Fluorescent Probes for Biological Imaging, School of Chemistry and Chemical Engineering, School of Materials Science and Engineering, University of Jinan, Jinan, Shandong 250022, P. R. China

\*E-mail: [weiyanglin2013@163.com](mailto:weiyanglin2013@163.com) (W. Lin); [WangQA@hnu.edu.cn](mailto:WangQA@hnu.edu.cn) (Q. Wang)

Electronic Supplementary Information (ESI) available: [details of any supplementary information available should be included here]. See DOI: 10.1039/x0xx00000x

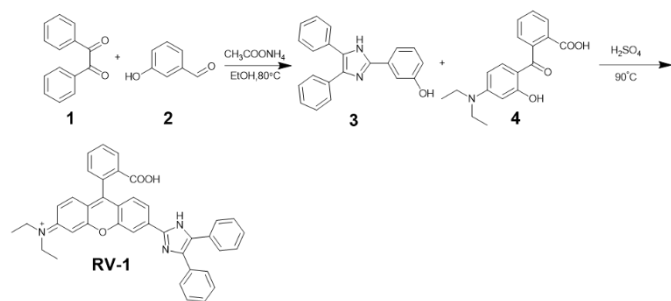
Rhodamine is a dye widely used as fluorescent probes for various analytes and laser source due to its excellent spectroscopic properties, such as long absorption and emission wavelengths, high fluorescence quantum yield, large extinction coefficient, and high stability against light.<sup>14–16</sup> However, most of the rhodamine derivatives have the absorption/emission wavelengths which are below 560/580 nm and show a small Stokes shift at the range of 10–30 nm, which may result in self-absorption and fluorescence detection error due to excitation backscattering effects.<sup>17,18</sup> Herein, we rationally designed and synthesized a new phenyl-substituted imidazole fused rhodamine dye **RV-1** with long absorption/fluorescence wavelengths, at about 573/655 nm, and a large Stokes shift about 82 nm (Scheme 1). We successfully utilized the probe **RV-1** for detection mitochondrial viscosity changes and zebra fishes. And more importantly, we applied the probe **RV-1** for monitoring viscosity variations in the inflammatory mice.

## Results and discussion

### Design and synthesis

The novel probe **RV-1** is consisted of two moieties, the 2, 3-dihydro-1H-xanthen core and the imidazole moiety which has two phenyl substituent groups. We envisioned that the imidazole moiety could serve as a molecular rotor because the imidazole moiety is connected to the 2, 3-dihydro-1H-xanthen core through a single bond, which could freely rotate. The single bond which connected the imidazole moiety and the 2, 3-dihydro-1H-xanthen core could cause a dark non-emissive excited state in low viscous media.<sup>7</sup> In contrast, these rotations could be hindered in high viscous media, leading to an enhancement of fluorescence emission. Furthermore, the restriction of these rotations may also render the whole molecule staying at the planar configuration in the charge transfer state, and forming a strong ICT system, which could cause a large Stokes shift.<sup>19</sup> Moreover, compared with the classic rhodamine B, the strong ICT system in **RV-1** may render it has longer absorption/emission wavelength than those of rhodamine B.

The probe **RV-1** was readily synthesized by a two-step reaction (Scheme 2). The structure of the probe was characterized by <sup>1</sup>H NMR, <sup>13</sup>C NMR, and high-resolution mass spectroscopy (HRMS, see ESI† for details).



Scheme 2 The synthesis of the probe **RV-1**.

### Optical response of probe **RV-1** to viscosity

To investigate the effects of viscosity to the new probe **RV-1**, various mixtures of methanol and glycerol with different volume

ratios which had varied viscosity were chosen as testing media. We first examined the absorption spectra of the probe **RV-1**. As shown in Fig. 1a, it had almost no absorption in methanol at above 500 nm. In contrast, a new absorption peaks at 573 nm appeared in 99 % glycerol. Then, the fluorescent emission spectra were also investigated. As shown in Fig. 1b, the probe exhibited almost no fluorescence above 600 nm when excited at 573 nm in methanol. This might be attributed to the free rotation between the imidazole ring and the 2, 3-dihydro-1H-xanthen core, which lead to a non-radiative decay of the excited state, weakening the fluorescent emission of the probe. Whereas, in the high viscous media, the free rotation of the imidazole moiety of the probe **RV-1** is hindered, which reduces the non-radiative pathway and restored the fluorescence emission. In addition, with the viscosity of the methanol-glycerol mixture gradually increasing from 0.6 to 953 cP, the fluorescent emission exhibits a remarkable increase (48.5-fold) when excited at 573 nm (Fig. 1c). Moreover, as shown in Fig. 1d, the probe shows a good linear relationship between the fluorescence intensity ( $\log I_{655}$ ) and viscosity ( $\log \eta$ ), ( $R^2 = 0.99$ ,  $x = 0.58$ ) by fitting the Förster–Hoffmann equation.<sup>20</sup> All of the above results indicate that **RV-1** has the potential to serve as an excellent probe for detection of viscosity changes.

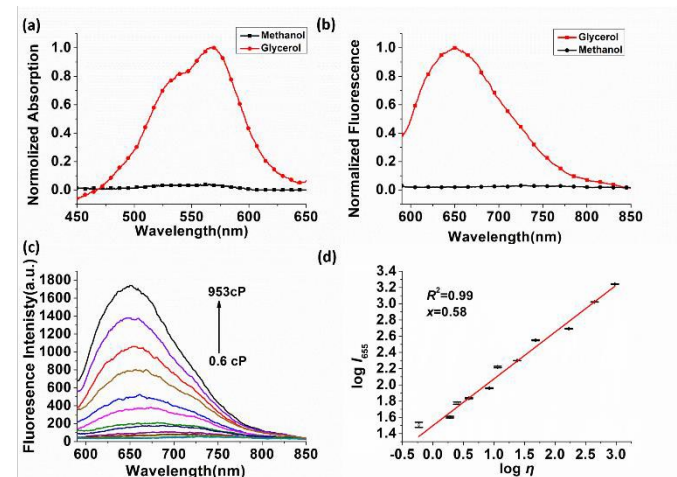


Fig. 1 (a) Normalized absorption of the probe **RV-1** in methanol and glycerol. (b) Normalized fluorescence emission of the probe **RV-1** in methanol and glycerol,  $\lambda_{ex}=570$  nm. (c) Fluorescence spectra of **RV-1** (10  $\mu$ M) with the variation of solution viscosity (methanol-glycerol system).  $\lambda_{ex}=570$  nm. (d) Linear relationship of  $\log I_{655}$  and  $\log \eta$ ,  $R^2 = 0.99$ ,  $x = 0.58$ .

We further measured the quantum yield of the probe **RV-1** in different solvents. As shown in Table 1, the quantum yield of the probe in other solvents was very low, in a range of 0.003–0.018. However, with the percentage of glycerol gradually increasing in methanol, the quantum yield of the solvents also increased, and reached to 0.116 in 99% glycerol. The above results indicated that the probe **RV-1** was sensitive to the viscous variations of the solvents.

The solvent polarity is an important factor which might influence the fluorescence of the probe. Because the cellular environment is very complex, it is hardly possible to distinguish the effect of viscosity on fluorescence or that from the polarity. Therefore, we measured the fluorescence spectra of the probe **RV-1** in solvents with different polarities to confirm that the probe **RV-1**

**Table 1** The photo-physical data of probe **RV-1** in different solvent systems

Solvents	Dielectric Constant	$\eta$ [a](cP)	$\lambda_{ab}$ (nm)	$\lambda_{em}$ (nm)	Fluorescence Quantum Yield
H <sub>2</sub> O	78.4	1.01	571	651	0.003
Dichloromethane	9.1	0.43	570	652	0.013
MeCN	37.5	0.37	573	653	0.016
Dioxane	2.2	1.54	568	650	0.015
THF	7.6	0.53	574	653	0.014
Acetone	20.7	0.32	571	652	0.018
Chloroform	5.1	0.54	568	650	0.013
DMSO	48.9	2.24	576	655	0.017
DMF	36.7	0.80	575	656	0.018
MeOH	32.6	0.59	573	655	0.015
MeOH/glycerol <sup>[c]</sup>	-	13.4	571	653	0.034
Glycerol	45.8	953	573	655	0.116

View Article Online

DOI: 10.1039/C8TB00298C

[a] The viscosity of the solvent; [b] Rhodamine B was used as a standard reference with a quantum yield of 0.97 in ethanol; [c] MeOH/glycerol=5:5, (v: v).

was independent of solvent polarity. As shown in **Fig.2**, the probe **RV-1** exhibits strong fluorescence emission in 99% glycerol. In contrast, in other solvents with different polarities, the probe **RV-1** has almost no fluorescence. These results indicate that the probe is not sensitive to the solvent polarity, and that it may be applied for monitoring viscosity changes in complex biological environments.

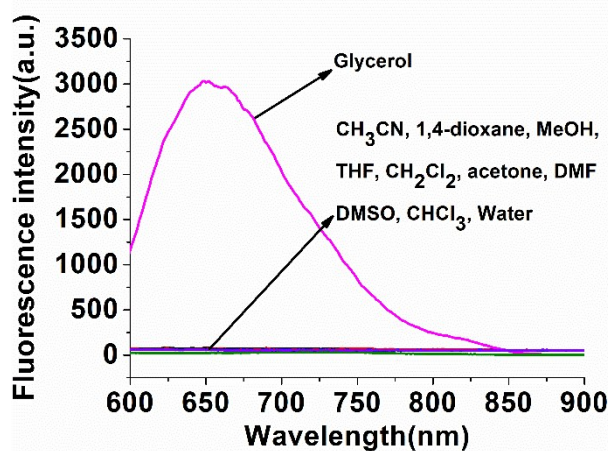


**Fig.2** Fluorescence emission of the probe **RV-1** in various solvents with different polarities.

### Fluorescence lifetime measurement

Because the fluorescence intensity may be influenced by the concentrations of the probe, we measured the fluorescence lifetime of the probe **RV-1**, as shown in **Table S1**, with the viscosity of the solvent systems increasing, the fluorescence lifetime gradually increased, which further indicated that the probe was sensitive to the viscosity changes of the solvents. Moreover, according to the Förster–Hoffmann equation,<sup>20</sup> as shown in **Fig. 3**, the fluorescence lifetime of the probe **RV-1** ( $\log \tau$ ) and viscosity ( $\log \eta$ ) exhibited a good linear relationship ( $R^2=0.99$ ,  $x=0.18$ ). These results further

proved that the probe **RV-1** could be rendered as a probe for measuring the viscosity changes of solvents.

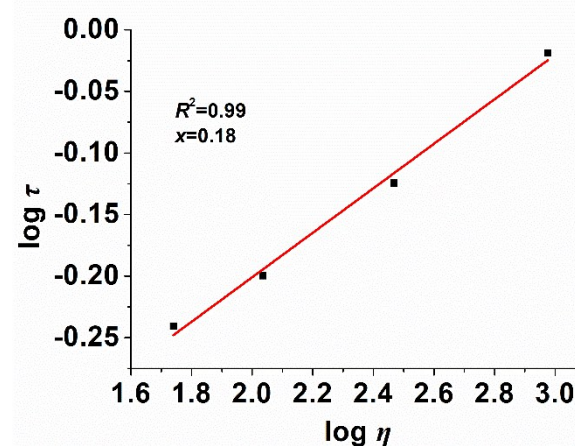


**Fig.3** Linear relationship of  $\log \tau$  and  $\log \eta$ ,  $R^2=0.99$ ,  $x=0.18$

### Theoretical Calculation and Mechanism

The structure of **RV-1** was optimized by DFT/TDDFT in B3LYP/6-31G (d) of Gaussian 09. As shown in **Fig.4a** and **FigS5**, the 2, 3-dihydro-1H-xanthene core and the imidazole moiety of **RV-1** stayed almost on a planar conformation, which caused the molecular structure of the probe **RV-1** in the optimal state displayed a large conjugated system. The frontier molecular orbitals in **Fig.4b** showed that in methanol, when the dihedral angle at around C13-C12-C53-N55 is either 0° or 90°, the HOMO centered at the imidazole moiety of **RV-1**, and the LUMO centered at the 2, 3-dihydro-1H-xanthene core. These phenomena demonstrate that the probe **RV-1** underwent an ICT process when excited from the ground state to the excited state, which rendered a large Stokes shift. Moreover, as shown in **Fig. 4a**, when the dihedral angle at around C13-C12-C53-

N55 is  $0^\circ$ , the oscillator strength  $f_{em}$  was 0.8259; when the dihedral angle at around C13-C12-C53-N55 is  $90^\circ$ , the oscillator strength  $f_{em}$  was only 0.0028 (Fig. 4b). These results indicated that the probe molecule could form a twisted excited state by intramolecular rotation, which led to weak non-fluorescence emission. From these calculation results, it was obviously that the probe **RV-1** could be rendered as a probe for detection of the viscosity changes of the solvents.

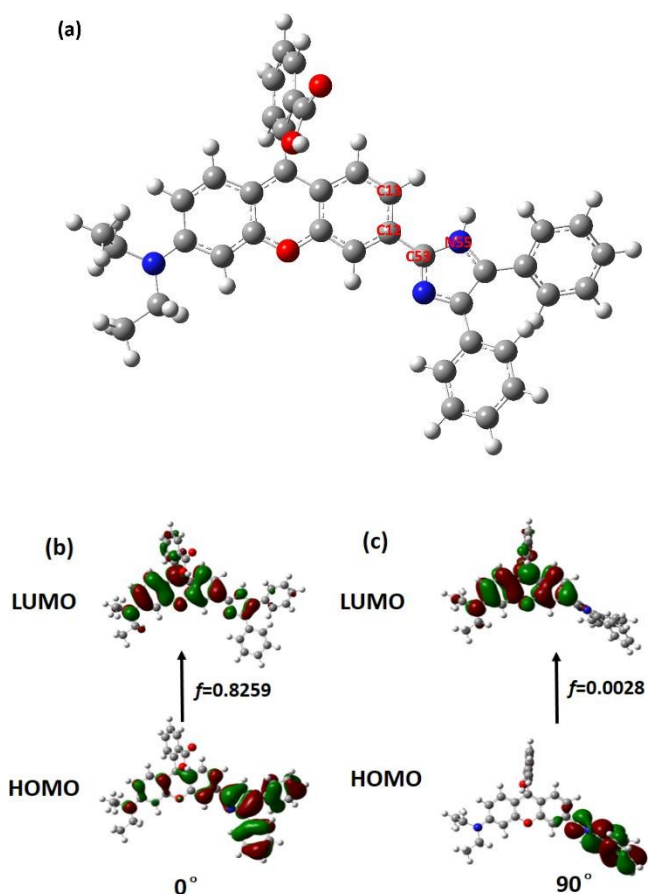


**Fig. 4** (a) The optimized geometries of **RV-1** in the excited states; (b) frontier molecular orbital of **RV-1** in the excited states with a dihedral angles of  $0^\circ$  at around C13-C12-C53-N55; (c) frontier molecular orbital of **RV-1** in the excited states with a dihedral angles of  $90^\circ$  at around C13-C12-C53-N55. Calculations were by the DFT method (PCM model) with a B3LYP/6-31G (d) basis set by using Gaussian 09.

#### Selectivity of probe **RV-1** to viscosity and pH dependence of the probe **RV-1**

The selectivity is a crucial requirement for fluorescent probes. Living cells are very complex, multicomponent systems, which contain numerous biological macromolecules such as proteins and DNA.<sup>21, 22</sup> These biological macromolecules might have crucial effect on the cellular viscosity. Moreover, cells contain various reactive oxygen species (ROS), reactive sulphur species (RSS), and ions, which may influence the probe **RV-1** in the complex biological system. Thus, we investigated the selectivity of **RV-1** for viscosity over DNA, BSA, ROS, RSS and various ions by fluorescence spectrometry (Fig. 5a). The addition of ROS, RSS and various ions didn't cause observable changes in the fluorescence emission of the probe **RV-1**, and

addition DNA or BSA to the solution of the probe **RV-1** only led to small enhancement of the fluorescence emission. These results showed that the fluorescence of the probe **RV-1** is not influenced by the biological macromolecules DNA, BSA, ROS, RSS, and ions.

Ring-opening form and lactone with different fluorescence properties are two forms of the rhodamine molecules.<sup>23-25</sup> At acidic conditions, the rhodamine derivatives stand on the ring-open forms, which usually have very strong fluorescence emission. In contrast, the rhodamine derivatives are on spirocyclic forms at basic conditions, which often have no fluorescence. Therefore, the fluorescence emission of rhodamine dyes is very sensitive to pH of solutions. Thus, we investigated the pH effect on the probe **RV-1**. As shown in Fig. 5b, the probe **RV-1** had stronger fluorescence emission at pH 4-7 than the fluorescence emission at pH 7-10, which could be attributed to the ring opening form in the acidic solutions. However, notably, all of the fluorescence emissions in PBS buffer solutions (Fig. 5b) are much lower than that in high viscous solutions (Fig. 2a). These data suggest that the probe **RV-1** could be applied for monitoring viscosity at physiological pH conditions.

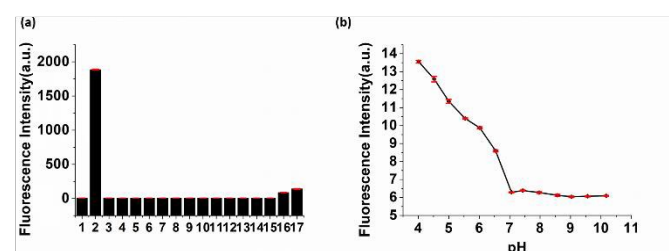


**Fig. 5** (a) 1. Fluorescence intensity of **RV-1** ( $10 \mu\text{M}$ ) at  $\lambda_{em} = 655 \text{ nm}$  in PBS buffer (pH=7.4, 0.01 mM); 2. Fluorescence intensity of **RV-1** ( $10 \mu\text{M}$ ) at  $\lambda_{em} = 655 \text{ nm}$  in 99% glycerol and various species ( $200 \mu\text{M}$ ). 1. blank; 2. 99% glycerol; 3. NaClO; 4. H<sub>2</sub>O<sub>2</sub>; 5. HO; 6. Cysteine(Cys); 7. Homocysteine(Hcy); 8. Glutathione(GSH); 9. Cu<sup>2+</sup>; 10. Zn<sup>2+</sup>; 11. Mg<sup>2+</sup>; 12. Fe<sup>3+</sup>; 13. Na<sup>+</sup>; 14. K<sup>+</sup>; 15. Ca<sup>2+</sup>; 16. DNA ( $200 \mu\text{L}$ ,  $100 \text{ mg/L}$ ); 17. BSA ( $200 \mu\text{L}$ ,  $100 \text{ mg/L}$ ). (b) pH effects on the probe **RV-1**.

#### Cell cytotoxicity assay and cell imaging

Cytotoxicity may influence the potential of a probe for application in living cell imaging. To determine the cytotoxic effect of the probe **RV-1**, we carried out the MTT experiment. The HeLa cells were incubated with **RV-1** (0, 1, 2, 5, 10, 15, 20, and  $40 \mu\text{M}$ ) for 24 h. As shown in Fig. S6 (ESI<sup>†</sup>), >90% HeLa cells survived after 24 h. The results indicate that the probe **RV-1** had low cytotoxicity and may be suitable for living cell imaging.

Monensin and nystatin could induce structural changes or swelling of mitochondria, which resulted in the mitochondria viscosity changes.<sup>26, 27</sup> As shown in Fig. 6, the cells treated with only the probe **RV-1** exhibited almost no fluorescence in the TRITC channel (570-620 nm). By contrast, when added Monensin or nystatin to the cells and stayed for 30 min, and then were incubated with the probe **RV-1** for another 30 min, the cells showed strong red fluorescence in the TRITC channel. The above results clearly suggest that the probe **RV-1** could be utilized to measure the viscosity variations in living cells.

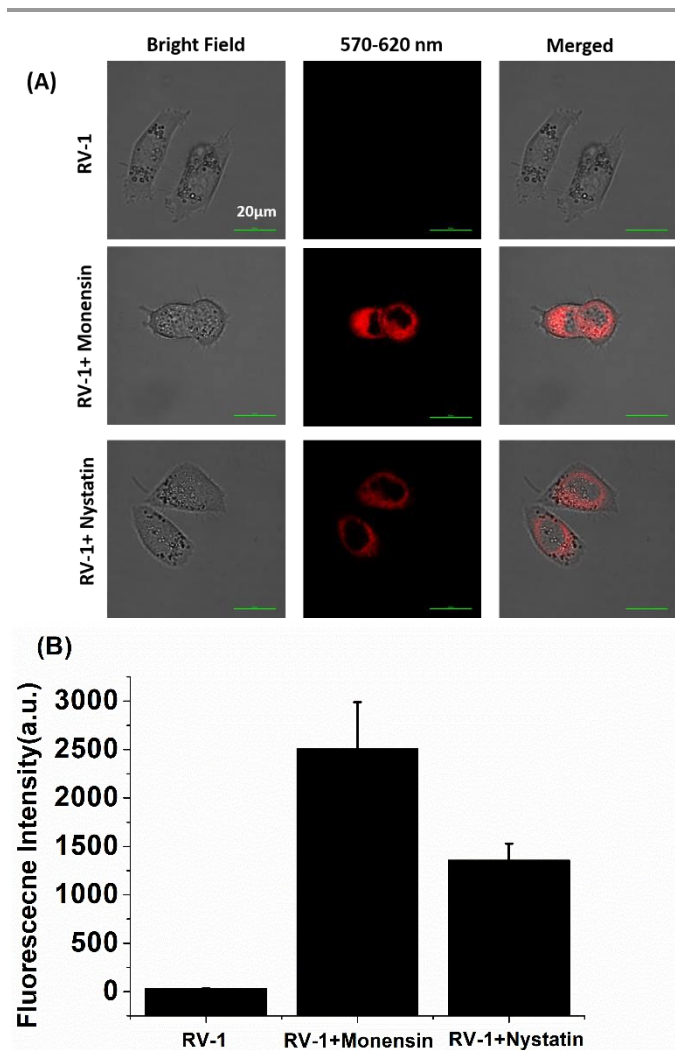


**Fig.6** (A) (a-c) Confocal fluorescence images of the HeLa cells incubated with 10  $\mu$ M free probe **RV-1** for 30 min; (d-f) Confocal fluorescence images of the HeLa cells incubated with 10  $\mu$ M probe **RV-1** + 10  $\mu$ M Monensin for 30 min. (g-i) Confocal fluorescence images of HeLa cells incubated with 10  $\mu$ M probe **RV-1**+10  $\mu$ M nystatin for 30 min. ; (B) Fluorescence intensity quantification. The images were collected in 570-620 nm, excited at  $\lambda_{ex}$ =561 nm, Scale bar = 20  $\mu$ m, Data are mean S.D. (bars) (n= 3).

Because the ring-open forms of the rhodamine dyes which possessed a positive charge delocalized through the whole molecular system often had the mitochondria-selectivity,<sup>28</sup> we expected that the probe **RV-1** also could be specifically localized on the mitochondria. To test the specificity of the probe **RV-1** for mitochondria, we carried out the co-localization experiment with the commercial mitochondria staining dye Mito-Tracker Green. As shown in **Fig. 7a**, the cells exhibited red fluorescence in the TRITC channel due to the emission of **RV-1**. At the same time, the cells showed green fluorescence in FITC channel owing to the emission of Mito-Tracker Green (**Fig. 7b**). The merged image (**Fig. 7c**) indicate that the two channels overlapped very well, and a high overlap coefficient of 0.935 was observed. The intensity profiles of **RV-1** and Mito-Tracker Green for region of interest (ROI) lines in HeLa cells also varied in close synchrony (**Fig. 7d**). Moreover, a high correlation was found in the intensity scatter plot of **RV-1** and Mito-Tracker

Green (**Fig. S7, ES†**), suggesting that the probe **RV-1** specifically exists on the mitochondria in the cells. DOI: 10.1039/C8TB00298C

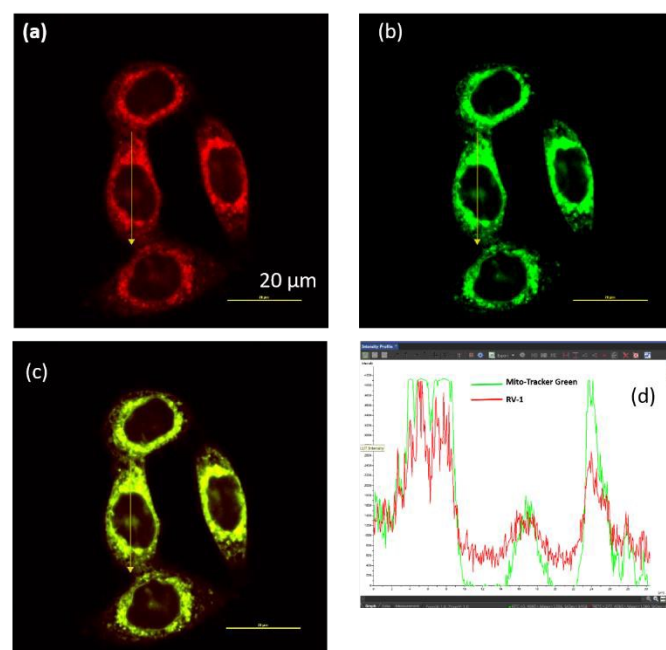


**Fig.7** (a-c) Confocal fluorescence images of the HeLa cells after incubation with 10  $\mu$ M probe **RV-1** + 10  $\mu$ M Nystatin and Mito-Tracker Green (10  $\mu$ M) at 37  $^{\circ}$ C for 30 min. (a) Fluorescence image from probe **RV-1** + 10  $\mu$ M Nystatin (b) Fluorescence image from Mito-Tracker Green; (c) The merged images; (d) The intensity profile of ROI lines. Scale bar = 20  $\mu$ m.

#### Fluorescence imaging in zebra fishes

Furthermore, we applied the probe **RV-1** for detection viscosity changes in zebra fishes.<sup>29</sup> As shown in **Fig. 8**, the zebra fishes only treated with the probe **RV-1** exhibited essentially no fluorescence in the TRITC channel (570-620 nm). When added Monensin or nystatin to the zebra fishes and stayed for 30 min, and then were treated with the probe **RV-1** for another 30 min, strong red fluorescence from the TRITC channel and was observed. These phenomena were consistent with the observations in the living cells, which further confirmed that the probe **RV-1** could be applied for detection of the viscosity changes in the living zebra fishes.

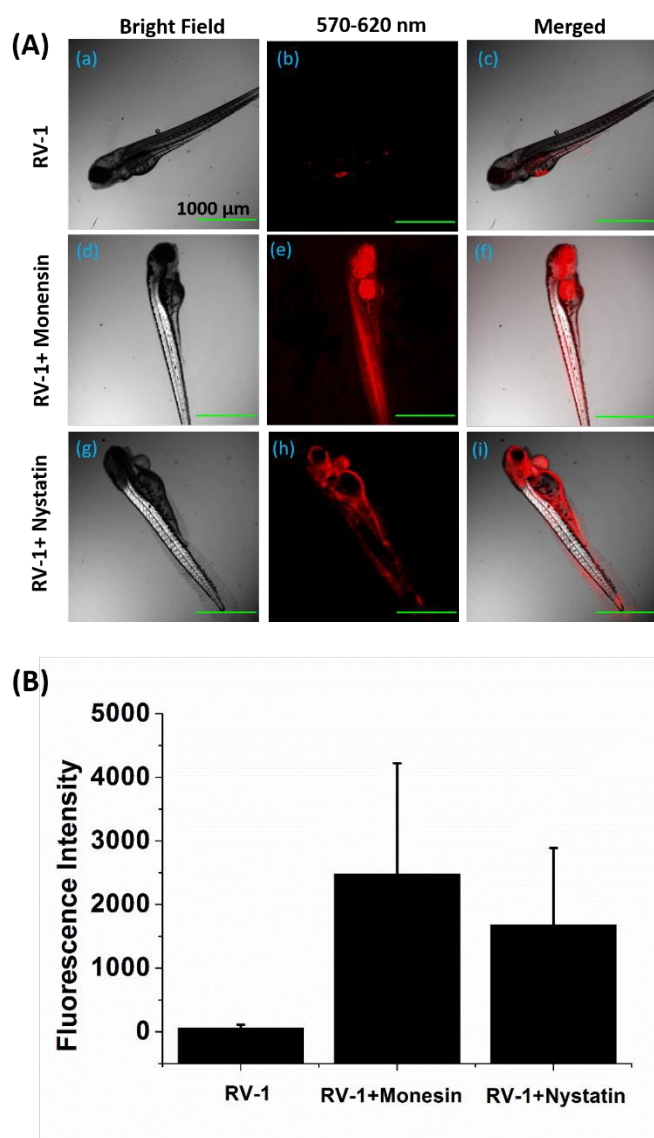


**Fig.8** (A) (a-c) Confocal fluorescence images of the zebra fishes incubated with 10  $\mu\text{M}$  probe RV-1 for 30 min; (d-f) Confocal fluorescence images of the zebra fishes incubated with 10  $\mu\text{M}$  probe RV-1+10  $\mu\text{M}$  Monensin for 30 min; (g-i) Confocal fluorescence images of zebra fishes treated with 10  $\mu\text{M}$  probe RV-1+10  $\mu\text{M}$  nystatin for 30 min. Scale bar =1000  $\mu\text{M}$ . (B) Fluorescence intensity quantification. The images were collected in 570-620 nm, excited at  $\lambda_{\text{ex}}=561$  nm, Scale bar = 20  $\mu\text{m}$ , Data are mean S.D. (bars) (n= 3).

### Fluorescence imaging in living mice

Lipopolysaccharide(LPS) has been reported that it could increase the blood viscosity of the rat<sup>30</sup>. Therefore we used LPS-injected mouse for imaging the blood viscosity changes *in vivo*. As shown in Fig.9, The healthy mice displayed essentially no fluorescence treated with RV-1. By contrast, the LPS-injected mice showed a very strong fluorescence emission, which displayed that the probe RV-1 could detection of blood viscosity changes in the LPS-injected mice.

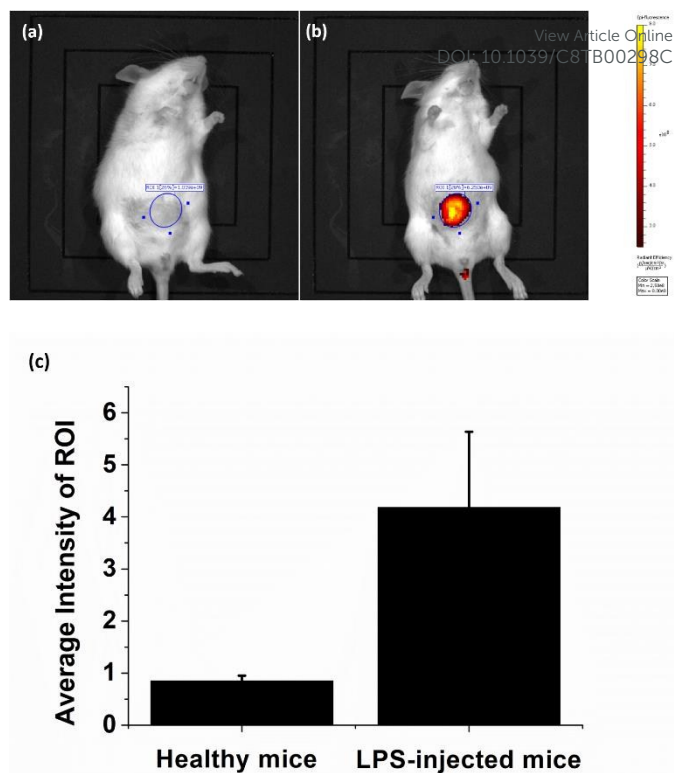


**Fig.9** (a) *In vivo* fluorescence imaging of viscosity in the living mice using RV-1. (a) 100 $\mu\text{L}$  of 10 $\mu\text{M}$  RV-1 was injected to healthy mice; (b) 100 $\mu\text{L}$  of 10 $\mu\text{M}$  RV-1 was injected to mice; (c) The relative average fluorescence intensity of ROI. Error bars represent standard deviation ( $\pm$ S.D.). n = 3, the statistical analysis was performed from three separate biological replicates.  $\lambda_{\text{ex}}=580$  nm,  $\lambda_{\text{em}}=660$  nm

### Conclusions

In summary, we have rationally designed phenyl-substituted imidazole fused rhodamine RV-1 as a new viscosity probe. The novel probe RV-1 showed a turn-on response to the viscosity with a long absorption wavelength at 573 nm and a large Stokes shift of 82 nm. RV-1 exhibited intense fluorescence emission at about 655 nm in 99% glycerol, with a very large, up to 48.5-fold enhancement of fluorescence intensity from methanol to 99% glycerol. Moreover, the probe RV-1 has been successfully applied for detection of the viscosity change in living cells and zebra fishes. More importantly, we used the probe RV-1 to monitor viscosity changes in living mice. We expect that the new probe RV-1 could be exploited as a powerful molecular tool for studying the critical role of viscosity changes in biological systems.

### Experimental

#### Preparation of the test solutions

Hydroxyl radical was generated by *in situ* by the Fenton reactions.<sup>31</sup> To 3 mL solution of RV-1 in H<sub>2</sub>O, hydrogen peroxide stock solution (120  $\mu\text{L}$ , 100 mM) was added. Aqueous Fe<sup>2+</sup> (60  $\mu\text{L}$ , 100 mM) was then added to the probe RV-1/H<sub>2</sub>O<sub>2</sub> solution to generate hydroxyl radical (200  $\mu\text{M}$ ). The

concentration of the solutions of NaClO, H<sub>2</sub>O<sub>2</sub>, cysteine(Cys), homocysteine(Hcy), glutathione(GSH), Cu<sup>2+</sup>, Zn<sup>2+</sup>, Mg<sup>2+</sup>, Fe<sup>3+</sup>, Na<sup>+</sup>, K<sup>+</sup>, Ca<sup>2+</sup> were 200 μM, the concentration of the solutions of BSA and DNA were 200 μL, 100 mg/L.

#### Measurement of Fluorescence lifetime

The fluorescence lifetime of the probe **RV-1** was measured by Edinburgh FLS920 Fluorescence Spectrometer. The concentration of the dye was 10.0 μM in various solvent mixture (methanol-glycerol solvent systems).

#### Measurement of fluorescence quantum yield (Φ)

Fluorescence quantum yield was determined by the relative comparison with Rhodamine B (Φ<sub>s</sub> = 0.97 in ethanol) as standard for **RV-1** in different solvents. And they were calculated by equation 1.<sup>32</sup>

$$\Phi = \Phi_s \frac{I_{A_s} \cdot \eta^2}{I_{sA} \cdot \eta_s^2} \quad (1)$$

In which, A is the absorbance, I is the integrated fluorescence intensity, and η is the refractive index of the solvent.

#### The Förster-Hoffmann equation

The relationship between the fluorescence emission intensity of the probe **RV-1** and the solvent viscosity could be formulated by the Förster-Hoffmann equation:<sup>20</sup>

$$\log I = C + x \log \eta \quad (2)$$

$$\log \tau = C + x \log \eta \quad (3)$$

Where η is the viscosity, I is the emission intensity, τ is the fluorescence lifetime of the probe, C is a constant, and x is the sensitivity of the probe to viscosity.

#### Theoretical calculations

All the calculations were performed with Gaussian09 program. The ground state structures of the compounds were optimized using time-dependent density functional theory (TD-DFT) by using a B3LYP/6-31G (d) level of theory. The solvent was methanol modeling with the polarizable continuum model (PCM).

#### Synthesis of RV-1

Compound **3** (614mg, 2.0mmol) and 2-(4-Diethylamino-2-hydroxybenzoyl) benzoic Acid (616mg, 2.0mmol) were dissolved in 3.0 ml 98% H<sub>2</sub>SO<sub>4</sub>, and was stirred at 90 ° C for 12h. Then, the mixture was cooled to room temperature, poured onto ice (200 g). The resulting precipitate was filtered off and washed with cold water (100 mL). Then the crude production was purified by silica gel flash chromatography using CH<sub>2</sub>Cl<sub>2</sub>/methanol (40:1) as eluent to afford compound **RV-1** as a dark purple solid (0.696g, 59%). <sup>1</sup>H NMR (400 MHz, Chloroform-d) δ 7.99 (d, J = 7.6 Hz, 1H), 7.88 (s, 1H), 7.62 (dt, J = 20.2, 7.3 Hz, 2H), 7.55 – 7.43 (m, 5H), 7.37 – 7.22 (m, 6H), 7.20 (d, J = 7.6 Hz, 1H), 6.69 (d, J = 8.3 Hz, 1H), 6.49 (d, J = 8.8 Hz, 1H), 6.37 – 6.26 (m, 2H), 3.30 (q, J = 7.1 Hz, 4H), 1.14 (t, J = 7.0 Hz,

6H). <sup>13</sup>C NMR (101 MHz, Chloroform-d) δ 170.13, 152.96, 151.94, 149.82, 144.75, 135.00, 131.88, 129.63, 128.70, 128.59, 128.29, 128.00, 127.36, 127.11, 124.98, 124.26, 120.36, 119.00, 114.06, 108.59, 104.75, 97.72, 44.45, 12.53. HRMS (ESI): m/z calculated for C<sub>39</sub>H<sub>32</sub>N<sub>3</sub>O<sub>3</sub><sup>+</sup> [M<sup>+</sup>], 590.2438, found 590.2438.

#### Conflicts of interest

There are no conflicts of interest to declare.

#### Acknowledgements

This work was financially supported by NSFC (21472067 and 21672083), Taishan Scholar Foundation (TS 201511041), and the startup fund of the University of Jinan (309-10004).

#### Notes and references

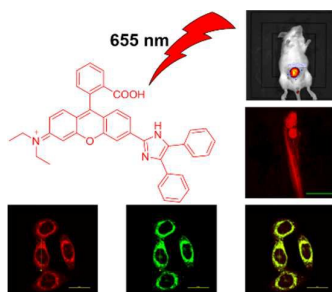
- 1 A. S. Verkman, *Trends Biochem. Sci.*, 2002, **27**, 27-33.
- 2 G. Guigas, C. Kalla and M. Weiss, *Biophys. J.*, 2007, **93**, 316-323.
- 3 K. Luby-Phelps, *Mol. Biol. Cell*, 2013, **24**, 2593-2596.
- 4 M. K. Kuimova, *Phys. Chem. Chem. Phys.*, 2012, **14**, 12671-12686.
- 5 H. Zhu, J. Fan, J. Du and X. Peng, *Acc. Chem. Res.*, 2016, **49**, 2115-2126.
- 6 I. Lopez-Duarte, T. T. Vu, M. A. Izquierdo, J. A. Bull and M. K. Kuimova, *Chem. Commun.*, 2014, **50**, 5282-5284.
- 7 M. A. Haidekker, M. Nipper, A. Mustafic, D. Lichlyter, M. Dakanali and E. A. Theodorakis, in *Advanced Fluorescence Reporters in Chemistry and Biology I: Fundamentals and Molecular Design*, ed. A. P. Demchenko, Springer Berlin Heidelberg, Berlin, Heidelberg, 2010, DOI: 10.1007/978-3-642-04702-2\_8, pp. 267-308.
- 8 M. L. Viriot, M. C. Carre, C. Geoffroy-Chapotot, A. Brembilla, S. Muller and J. F. Stoltz, *Clin. Hemorheol. Microcirc.*, 1998, **19**, 151-160.
- 9 M. K. Kuimova, in *Molecules at Work: Selfassembly, Nanomaterials, Molecular Machinery*, Wiley-VCH Verlag GmbH & Co. KGaA, 2012, DOI: 10.1002/9783527645787.ch11, pp. 243-262.
- 10 M. A. Haidekker, T. P. Brady, D. Lichlyter and E. A. Theodorakis, *J. Am. Chem. Soc.*, 2006, **128**, 398-399.
- 11 L. Wang, Y. Xiao, W. Tian and L. Deng, *J. Am. Chem. Soc.*, 2013, **135**, 2903-2906.
- 12 Z. Yang, Y. He, J.-H. Lee, N. Park, M. Suh, W.-S. Chae, J. Cao, X. Peng, H. Jung, C. Kang and J. S. Kim, *J. Am. Chem. Soc.*, 2013, **135**, 9181-9185.
- 13 Y. Baek, S. J. Park, X. Zhou, G. Kim, H. M. Kim and J. Yoon, *Biosens. Bioelectron.*, 2016, **86**, 885-891.
- 14 L. Yuan, W. Lin, K. Zheng and S. Zhu, *Acc. Chem. Res.*, 2013, **46**, 1462-1473.
- 15 L. D. Lavis, *Annu. Rev. Biochem.*, 2017, **86**, 825-843.
- 16 M. Beija, C. A. M. Afonso and J. M. G. Martinho, *Chem. Soc. Rev.*, 2009, **38**, 2410-2433.
- 17 X. Peng, F. Song, E. Lu, Y. Wang, W. Zhou, J. Fan and Y. Gao, *J. Am. Chem. Soc.*, 2005, **127**, 4170-4171.

## ARTICLE

## Journal Name

- 18 W. Lin, L. Yuan, Z. Cao, Y. Feng and J. Song, *Angew. Chem. Int. Ed.*, 2010, **49**, 375-379.
- 19 F. Vollmer, W. Rettig and E. Birckner, *Journal of Fluorescence*, 1994, **4**, 65-69.
- 20 M. A. Haidekker and E. A. Theodorakis, *J. Biol. Eng.*, 2010, **4**, 11.
- 21 G. L. Lukacs, P. Haggie, O. Seksek, D. Lechardeur, N. Freedman and A. S. Verkman, *J. Biol. Chem.*, 2000, **275**, 1625-1629.
- 22 D. S. Banks and C. Fradin, *Biophys. J.*, 2005, **89**, 2960-2971.
- 23 R. Wang, C. Yu, F. Yu, L. Chen and C. Yu, *TrAC, Trends Anal. Chem.*, 2010, **29**, 1004-1013.
- 24 L. Yuan, W. Lin, Y. Yang and H. Chen, *J. Am. Chem. Soc.*, 2012, **134**, 1200-1211.
- 25 M. H. Lee, J. H. Han, J. H. Lee, N. Park, R. Kumar, C. Kang and J. S. Kim, *Angew. Chem. Int. Ed.*, 2013, **52**, 6206-6209.
- 26 A. C. Souza, F. S. Machado, M. R. N. Celes, G. Faria, L. B. Rocha, J. S. Silva and M. A. Rossi, *Journal of Veterinary Medicine Series A*, 2005, **52**, 230-237.
- 27 S. P. Soltoff and L. J. Mandel, *J. Membr. Biol.*, 1986, **94**, 153-161.
- 28 B. C. Dickinson, D. Srikun and C. J. Chang, *Curr. Opin. Chem. Biol.*, 2010, **14**, 50-56.
- 29 P. Ning, P. Dong, Q. Geng, L. Bai, Y. Ding, X. Tian, R. Shao, L. Li and X. Meng, *J. Mater. Chem. B*, 2017, **5**, 2743-2749.
- 30 E. Yeom, H. M. Kim, J. H. Park, W. Choi, J. Doh and S. J. Lee, *Sci. Rep.*, 2017, **7**, 1801.
- 31 H. J. H. Fenton, *J. Chem. Soc., Trans.*, 1894, **65**, 899-910.
- 32 Benniston, A. C.; Clift, S.; Harriman, A. *J. Mol. Struct.* 2011, **985**, 346-354.

View Article Online  
DOI: 10.1039/C8TB00298C



We designed a novel mitochondria-targeted rhodamine analogue for detection of viscosity changes in living cells, zebra fishes, and living mice.